doi:10.3788/gzxb20174605.0532001

少周期飞秒准径向偏振光的超快瞬变聚焦矢量场

张远达[1,2],李修建[1],贾辉[1],聂永明[3],刘希顺[4]

(1 国防科学技术大学 理学院,长沙 410073)

(2 95975 部队,甘肃 酒泉 732750)

(3 中国卫星海洋测控中心,江苏 江阴 214431)

(4 国防科学技术大学 电子科学与工程学院,长沙 410073)

摘 要:研究了基于腔外螺旋相位调制获取高峰值功率飞秒准径向偏振光的方法,结果表明该方法所产生的并非完全纯净的径向偏振光,其径向分量决定了聚焦后纵场的分布,而径向和角向分量共同影响了横场的分布.根据 Richard-Wolf 矢量衍射理论模拟得到不同纯度下的少周期飞秒准径向偏振光在焦点附近的电场的时空矢量分布,发现其具有中心对称和震荡衰减特点,载波包络相位将对聚焦场的矢量时空分布产生显著影响,从而对飞秒脉冲与电子在聚焦场中的相互作用产生影响.研究结果可为进一步的激光粒子加速分析以及偏振转换器的设计提供依据.

关键词:准径向;少周期;快变;矢量;聚焦;模拟

中图分类号:O438 **文献标识码**:A **文章编号**:1004-4213(2017)05-0532001-9

Ultrafast Transient Focal Vector Field of Few-cycle Femtosecond Quasi Radially Polarized Beams

ZHANG Yuan-da[1,2], LI Xiu-jian[1], JIA Hui[1], NIE Yong-ming[3], LIU Xi-shun[4]

(1 *College of Science, National University of Defence Technology, Changsha* 410073, *China*)

(2 *PLA Unit* 95975, *Jiuquan, Gansu* 732750, *China*)

(3 *China Satellite Maritime Tracking and Controlling Department, Jiangyin, Jiangsu* 214431, *China*)

(4 *Colleges of Electric Science and Technology, National University of Defence Technology, Changsha* 410073, *China*)

Abstract: The extra-cavity quasi-continue spiral phase modulation method for generating high peak power quasi- radially polarized beam was studied, which show that the generated beam is not perfect radially polarized, the radially polarized components determine the longitudinal electric field distribution, and the transversal field distribution is determined by both of the radially and the azimuthally polarized components. Considering the Richard-Wolf vector diffraction theory, the spatial and temporal distribution of the electric field vectors around the focal spot for various purities were simulated. The results show that the spatial and temporal distribution possesses the features of centrosymmetry and oscillation attenuation, and will be remarkably affected by the carrier envelope phase. Furthermore, the analysis indicates that the interactions between the focused pulse and the electron will be significantly determined by the spatial and temporalvector distribution at the focal spot. The results will provide valuable basis for the laser-particler interaction analysis and further polarization convertor designs.

Foundation item: The National Natural Science Foundation of China (Nos. 61070040, 61108089, 61205087, 61107005)

First author: ZHANG Yuan-da (1989—), male, assistant engineer, M. S. degree, mainly focus on information optics. Email: zyd04333281256@163.com.

Corresponding author: LI Xiu-jian (1974—), male, professor, Ph. D. degree, mainly focuses on information optics, ultrafast optics and optical computing. Email: xjli@nudt.edu.cn

Received: Nov. 15, 2016; **Accepted**: Feb. 23, 2017

Key words: Quasi-radially; Few-cycle; Transient; Vector; Focusing; Simulation
OCIS Codes: 320.7120; 320.7160; 140.3430; 140.3460

0 Introduction

Analysis on the laser-particle interactions is drawing increasing attentions because of its wide prospective applications on various fields. And with super strong longitudinal components and sharp focal spot under the high Numerical Aperture (NA) focusing apparatus, the radially polarized beam has a promising prospect in laser-particle interactions[1]. Few-cycle femtosecond Radially Polarized Beams (RPBs) may just help to achieve excellent laser-induced electron acceleration with laser pulse peak-power higher than peta-watt[2]. Generally, the high peak power is the most special character of the femtosecond pulse. Actually, the concerning interactions just lie to the longitudinal electric field to the charged particles, such that the polarized beams should be focused to obtain the longitudinal electric field along the optical length and promote the transient laser power to enhance the interactions[3]. In comparison with the uniformly polarized beams, the RPBs show an excellent focusing quality[4-6]. When being focused, the Linearly Polarized Beam (LPB) possesses the effective longitudinal component along the optical axis, and obviously brings about the transversal component that could lead to the extra and useless drift of the particles[7]. While for the RPBs, there is a fairly strong longitudinal superposition and no transversal component at the axle, which is paramount for the laser-particle interactions[8-9].

Besides, to utilize the super-high peak power, the femtosecond pulse should be temporally short enough and therefore, the light oscillation is transient[10-11]. Thus, the vector distribution at every moment and position is indispensable for the analysis to the mutual effects, such as the laser parameter designing and the accelerating field layout, etc. In this way, the discussion on ultrafast transient focal vector field of few-cycle femtosecond quasi RPBs is of great significance.

Meanwhile, how to sufficiently generate high pure few-cycle RPBs is the premise for the applications. Usually, for both intra-cavity and extra-cavity converting methods[12-14], the generated RPBs are not completely pure in radial polarization rather than quasi. This will affect the imperfect focusing features, especially the spatial and temporal vector field of the focal spot which further influence its wide applications[15-16]. Ref. [17] gives some focusing results involving various radial polarization purities which are the superposition of uniform Radially Polarized (RP) and Azimuthally Polarized (AP) beams.

However, the spatial and temporal vector field of the focal spot has not been analyzed for the few-cycle femtosecond conditions, which will be different from that of the CW. This paper will try to obtain the few-cycle femtosecond quasi-RPB, and discuss its ultrafast transient focal vector field by various RP purities and the interaction features with the electron at the spot, so as to reveal the details and the advantages of the spatial and temporal focal vector field.

1 Quasi-RPBs based on quasi-continue spiral phase modulation

1.1 Design of the generator

On the basis of the system raised by Qi Jun-li [18], the polarization rotation can be achieved by crystal-type SLM. Considering the Jones Matrix of the SLM is

$$\boldsymbol{J}(\delta)=\begin{bmatrix}1 & 0\\ 0 & \mathrm{e}^{\mathrm{i}\delta}\end{bmatrix} \tag{1}$$

where, δ stands for the phase retardation caused by the different voltage value electric field applied on the liquid crystal (x, y), which can modulate the phase retardation in different areas. Then, with two concerning quarter wave plates whose fast-axles directions are orthogonal, 45° and 135° respectively, the angle of rotation of certain point can be controlled finely, and the Jones Matrix of the converting set is shown as

$$\boldsymbol{J}=\mathrm{e}^{\mathrm{i}\frac{\delta(x,y)}{2}}\begin{bmatrix}\cos\dfrac{\delta(x,y)}{2} & \sin\dfrac{\delta(x,y)}{2}\\ -\sin\dfrac{\delta(x,y)}{2} & \cos\dfrac{\delta(x,y)}{2}\end{bmatrix} \tag{2}$$

When the LPB passes through the system, the polarization direction will be rotated by any angle according to the retardation value. Further, some crystals can meet the requirements of the phase retardation function of the SLM, such as the birefringence crystals and the wave plates, of which the $YbVO_4$ and the silica are typical.

In aspect of the birefringence, the value of the $YbVO_4$ crystal is much larger than that of the silica ($N_e - N_o = 0.214 \sim 0.009$@800 nm). As for the roto-optic effect of silica, to achieve the rotation angle of 360°, the thickness should be as large as 31.5 mm ($\alpha = 11.44°/\text{mm}$@800 nm), which makes it hard to splice the wave plate. Thus, the phase modulation based on birefringence is preferred. The $YbVO_4$ crystal possesses a fine transmittance in a large range spectrum including the visible and the near infrared spectrums. The corresponding laser Damage Threshold (DT) is higher than 15 J/cm^2@10 ns, and the transmission loss is less than 0.1%/cm^{-1}.

According to Eq. (2), the high power femtosecond quasi-RPBs with pulse duration of few-cycle are converted from LPBs[12,19] by converters whose structures can be shown as Fig. 1 (a), i.e., in 3-D helical sector-shape. The sub-section beam from any sector will not be completely radially polarized, but linearly in a certain direction at the whole sector respectively, as shown in Fig. 1 (b).

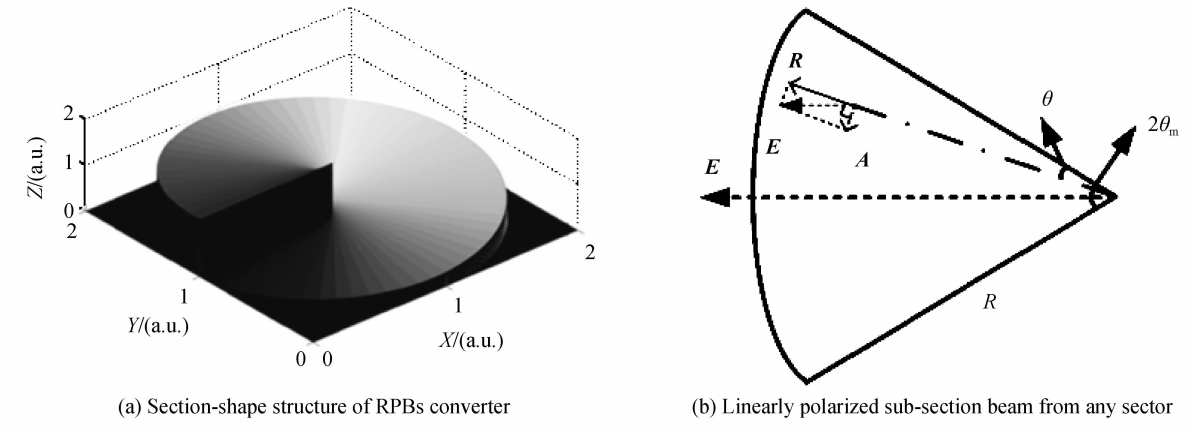

(a) Section-shape structure of RPBs converter (b) Linearly polarized sub-section beam from any sector

Fig. 1 RPBs converter and sub-section beam

Correspondingly, the phase compensator is also shown in Fig. 2, which should meet the requirement to offset the phase difference caused by the varied optical length, as

$$\Delta\delta_1 + \Delta\delta_2 = \text{Const} \tag{3}$$

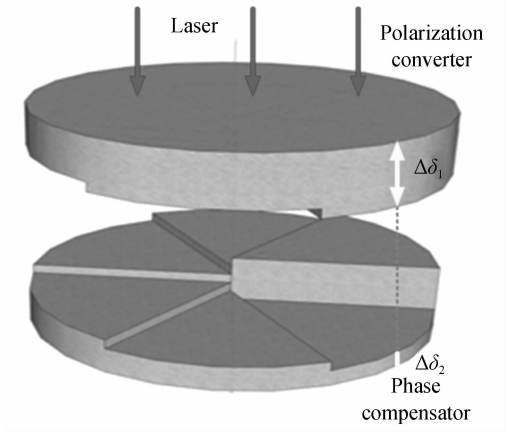

Fig. 2 Principle of the phase compensation

According to the Sellmeier Function, the birefringence of $YbVO_4$ is 0.214 ($n_o = 1.972$, $n_e = 2.186$). And the phase retardation value is proportional to the thickness, as

$$\delta(\theta) = \frac{2\pi[n_o - n_e]d(\theta)}{\lambda} \tag{4}$$

To meet the polarization rotation from 0 to 2π, the value of $\delta(\theta)$ is $0 \sim 4\pi$, and the fabricating thickness is $0 \sim 7.484$ μm. For the compensator, assuming the index of the silicon is n_{SiO_2}, the

corresponding thickness is

$$d=\frac{m\lambda}{n_{SiO_2}-1} \quad (m=1,2,\cdots) \tag{5}$$

Overall, the generator is consisted with two quarter wave plates, a spiral-like structure with the $YbVO_4$ crystal and a concerning phase compensator made by silicon, so as to obtain the high peak power RPBs.

1.2 Purity of quasi-RPBs

Generally, the obtaining can be considered as the superposition of RP and AP beams, in which the proportion of the RP beams is regarded as the purity of the RP[17]. For any sub-section beam from a sector with cross scheme as shown in Fig. 1 (b), the linearly polarized vector can be always orthogonally decomposed to radially polarized vector and azimuthally polarized vector. When being focused, the AP components will not affect the focusing electric intensity and vector amplitude in longitudinal.

Assuming that the beam is uniform and normalized in intensity over the whole cross section, that is, $\boldsymbol{E}_r=\boldsymbol{E}_R$ for a sector with fan angle of $2\theta_m$, the Equivalent Radially Polarized Portion (ERPP) at one point is $f(r,\theta)=1\times\cos\theta$. And the whole results of the beam can be expressed as

$$S=2\int_0^{R}\int_0^{\theta_m} f(r,\theta)(r\mathrm{d}\theta)\mathrm{d}r=R^2\sin\theta_m \tag{6}$$

And the corresponding radial polarization purities ρ is calculated as

$$\rho=\frac{S}{S_0}=\frac{\sin\theta_m}{\theta_m} \tag{7}$$

where

$$S_0=\frac{2\theta_m}{2\pi}\pi R^2=\theta_m R^2 \tag{8}$$

To make the definition of the purity universal, the convergence angles φ of the radius which causes the ERPP different can be considered as $f_\varphi(r,\theta)$ at (r,θ).

$$f_\varphi(r,\theta)=\cos\theta\sin\varphi \tag{9}$$

where, φ varies from 0 to φ_m, and φ_m is the maximum convergence angle. Thus, the expressions of S and S_0 can be reconsidered due to this angle, but since the value of φ is only relevant with r, the purity doesn't change.

Similarly in Fig. 1 (b), the Equivalent Azimuthally Polarized Portion (EAPP) in the transversal direction could be expressed as

$$f_a(r,\theta)=\cos\theta\cos\varphi+\sin\theta \tag{10}$$

which can be regarded as the effects caused by APB equivalently.

More generally, when the expressions with radius r and angle θ in EP or the intensity distributions cannot be separated as Eq. (6), the results of the purity could be much more complex, such as the Gaussian intensity envelop.

1.3 Influences of quasi-continue structures on laser beam properties

Actually, as shown in Fig. 3, the quasi-continue structure contains numerous tiny steps, which can induce some factors that can affect the focusing. When the step number increases, the purity of the gained RPB in theory is also improved.

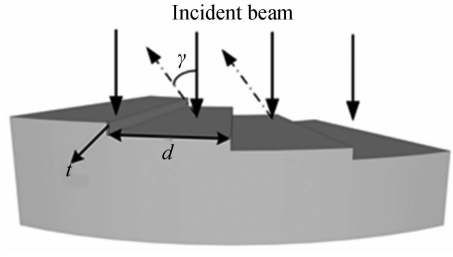

Fig. 3 Schematic of the Michelson echelon

1.3.1 *Considering on the diffraction effects*

The mutational interfaces between the steps are inevitable, so the diffraction effects would occur to distort the wave front and it also causes the deviations of propagation for portions of the light which will reduce the laser beam quality. Thus, the interfaces are paramount for the effects of the diffraction.

The model of the spiral steps can be analyzed as reflection-type Michelson echelon, which is made up of numbers of parallel crystal plates, shown as Fig. 3. As the plates are of the same refractive index, when irradiated by the parallel incident beam, the spiral steps will have the diffraction effects just like that of

multiple-slits.

While, the fairly low reflecting index of the $YbVO_4$ crystal, as small as 8% (@ 800nm), would obviously decrease the potential diffraction effects. And the mere 8% part is discussed below.

When the diffraction angle θ as shown in Fig. 3 is small enough, the optical length difference between the two adjacent steps can be estimated as $\Delta \approx 2t$, where t is the height of the step. Actually, for the ion etching method employed, the step height is about 10 nm, which is about one order smaller than that of the central wavelength 800 nm. Considering the coherent phenomena on the interface, the phase difference of the two sides is about $\frac{\pi}{20}\left(=\frac{10\times 2}{800}\times 2\pi\right)$, which indicates that the diffraction here can be negligible at the near-field. Unlikely, the height between the first and the last step is about 7.4 μm, which should be concerned for the superposition to the diffraction. The corresponding optical phase difference is about $\frac{37\pi}{2}$ $\left(\frac{7400\times 2}{800}\times 2\pi\right)$, which donates nearly nothing to the intensity increase by the superposition of the electric fields. Besides, it is only one of the numerous interfaces, making little difference to the whole. Thus, the steps can be treated as the roughness of the plane. In fact, the optical efficiency is somehow reduced due to this structure.

1.3.2 *Considering on the pulse duration change*

Assuming that the laser pulse intensity is moderate enough and cannot cause any nonlinear effects in the crystals, the dispersions would change the pulse duration differently for various thicknesses. For an incident laser pulse with a Gaussian profile, the results can be expressed as

$$A(t)\exp\{\mathrm{i}\varphi(t)\}=A_0\exp\left[-4\ln 2(t/\tau_\mathrm{p})^2/2\right] \tag{11}$$

$$\tau_{\mathrm{p,out}}=\left[1+a_0\varphi''^2/(\tau_\mathrm{p})^4\right]^{1/2}\cdot\tau_\mathrm{p} \tag{12}$$

where, τ_p is the Full Width at Half Maximum (FWHM) of the input pulse, the pulse duration after passing through the crystal can be calculated by Eq. (12), in which $a_0=(4\ln 2)^2$, φ'' is the 2nd-order Group Velocity Dispersion (GVD), $\varphi''(\bar{\omega})=-k''(\bar{\omega})z$ and $k(\bar{\omega})=\frac{\bar{\omega}n(\bar{\omega})}{c}$.

The relationship between the medium length z and the pulse duration $\tau_{\mathrm{p,out}}$ can be obtained. Consequently, the pulse will be stretched in temporal width, which leads to the decrease of the peak power. Actually, for the pulse with central wavelength of 800 nm and pulse duration of 50 fs, the GDD for SiO_2 is as weak as almost 75/fs^2 per millimeter. When the pulse passes through the crystal with a thickness of 6 μm, the fairly small changes of the pulse duration, calculated as Eq. (13), can be neglected. It is also the same with $YbVO_4$.

$$\tau_{\mathrm{p,out}}=(1+2.423\times 10^{-12})^{1/2}\cdot\tau_\mathrm{p} \tag{13}$$

Thus, the impacts of the dispersion on the pulse duration and peak power can be ignored. In practical fabrication, there must be a basement of a certain thickness beneath the spiral step structure, about several millimeters, which is much thicker than the valid polarization rotation portion's size by two or more magnitudes. Therefore, the basement is regarded as conducting the same pulse stretching effects all around, which indicates that extra compensation would not be necessary at this aspect.

1.3.3 *Considering on the wavelength dependence*

According to Eq. (4), the maximum machining depth can be estimated as $d(2\pi)=2\lambda/\Delta n$, and then the relationship between the depths and the wavelengths can be obtained as Fig. 4 for $YbVO_4$.

It is shown that the machining depth is nearly linearly relevant with the wavelength, such that the dispersion effects should be concerned. Take 800 nm wavelength as an example, in order to achieve adequate phase modulation, the depth change should be from 0 to 7.484 μm.

Precisely, in each sector, the polarization directions of the central frequency are all the same as that of the angle bisector. However, their directions would suffer some fixed deflections, shown as Fig. 5, which depicts the diagram of the polarization distributions in a sector, assuming the central angle is $2\alpha_0$ and the deflecting angle is β. When the depth is 7.484 μm, in comparison with the wavelength of 0.8 μm, β are 0.807 3° and −0.635 5° respectively for the wavelength 0.72 μm and 0.88 μm. The results could be smaller for other wavelengths and depths.

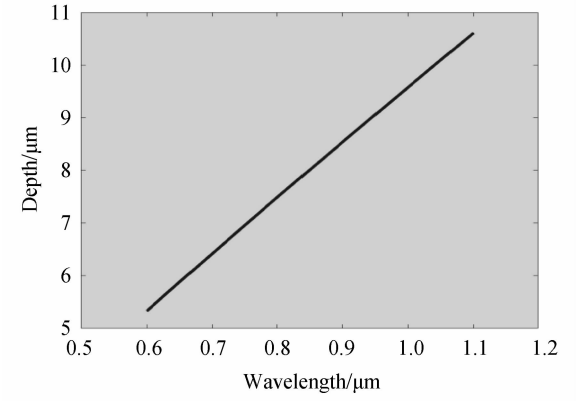

Fig. 4 Relations between the depth and wavelength

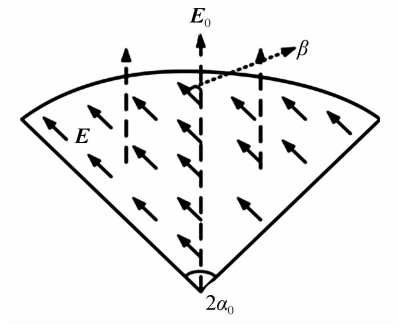

Fig. 5 Deflection of the polarization directions

It can be indicated that the purity for certain frequency whose polarization directions possess a deflecting angle β, is similar to that of the central frequency when β is small enough, calculated by Eq. (14), where p represents the purity of the RP part. Thus, the error induced by wavelength can be ignored.

$$p=\frac{\sin\alpha_0\cos\beta}{\alpha_0} \tag{14}$$

Actually, the process of the ion etching technology is conducted on the backing material, not same as the traditional crystal-splicing, such that there will be little physical effects caused by the energy deposit within the interfaces.

2 Focusing simulations of the few-cycle femtosecond Quasi-RPB

It should be highlighted that for the focusing of this kind of uneven polarized beams in this paper, off-axis parabolic reflector is concerned with which the dispersion effects could be neglected.

Based on the vectorial diffraction theory of Richard-Wolf which is responsible for the focusing of a paraxial optical field by aplanatic optical devices, and considering that the quasi RPB electric field has varied distributions at the entrance pupil, i. e. , with different purity, the modeling of the focusing electric field can be conducted as[20]

$$E(r_{\mathrm{P}},\varphi_{\mathrm{P}},z)=-\frac{\mathrm{if}}{2\pi}\iint_{\Omega}\sqrt{\cos\varphi}\,\frac{L\cdot E_0(k_r,k_\varphi)}{k_z}\mathrm{e}^{\mathrm{i}k_{\mathrm{r}}r_{\mathrm{P}}\cos(k_\varphi-\varphi_{\mathrm{P}})+\mathrm{i}k_z z}k_{\mathrm{r}}\,\mathrm{d}k_{\mathrm{r}}\,\mathrm{d}k_\varphi \tag{15}$$

where, $E(r_{\mathrm{P}},\varphi_{\mathrm{P}},z)$ is the electric field at a point P on the collecting plane $(r_{\mathrm{P}},\varphi_{\mathrm{P}},z)$, and $(k_{\mathrm{r}},k_\varphi,k_z)$ is the components of the wave vector k, $E_0(k_{\mathrm{r}},k_\varphi)$ is the distribution at the entrance pupil, φ represents the divergence angle, L is the divergence matrix, f stands for the equivalent focal length, respectively. By integrating over the whole cross section of the beam, i. e. Ω, the simulation results of quasi-RPBs are shown in Fig. 6. In simulations, the NA=0.9 and the central wavelength is 800 nm.

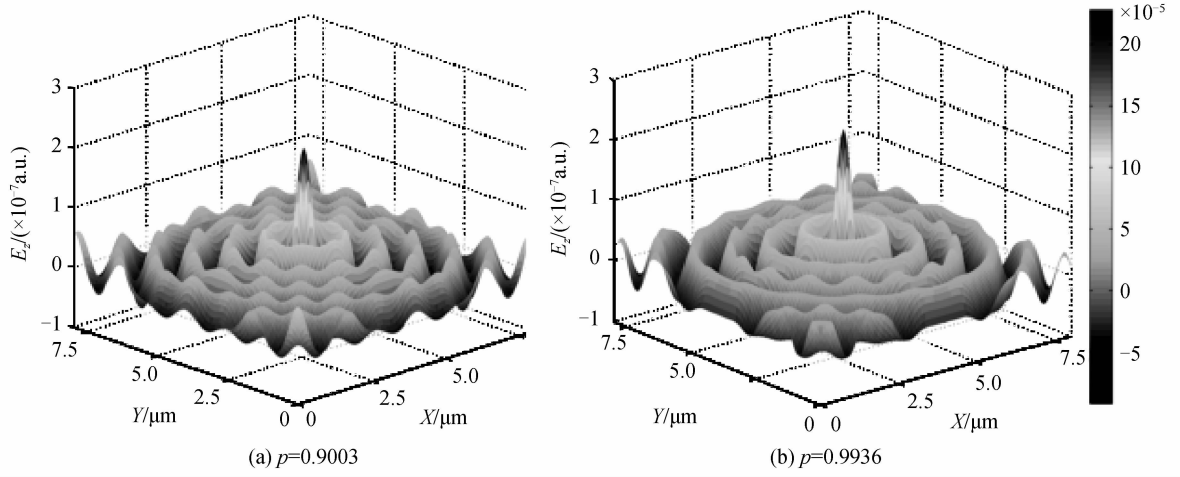

Fig. 6 Longitudinal component vector amplitude distributions at focal plane of different purities

It should be figured out that the longitudinal electric field has a periodical change at the focal plane, and that the intensity gets to the peak at the spot. When the purity is higher, the longitudinal intensity could be stronger (2.027×10^{-7} vs. 2.283×10^{-7} in Fig. 6).

Also, in Fig. 7, the stronger peak intensity of higher purity can be seen, and the FWHM of c is smaller than that of d(0.7 μm vs. 0.9 μm), which derives from the different focusing extent of longitudinal field and that the RP components determine the longitudinal electric field.

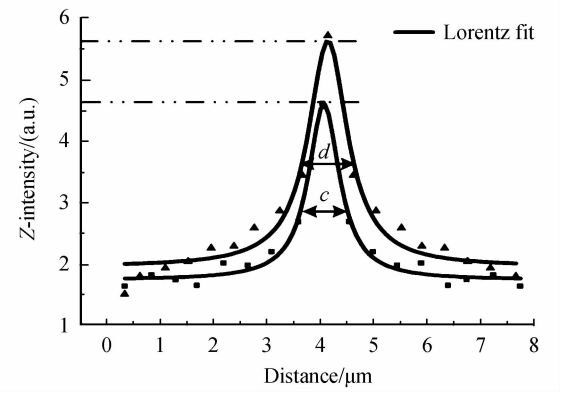

Fig. 7 Intensity distributions of the cross profile through the spot in Fig. 6

On the other hand , the transversal electric field is also affected by the purity. The peak power in e is 9.744×10^{-14}, while in f, the value is mere 6.685×10^{-14}. As shown in Fig. 9, the envelope of e has a larger FWHM than f(2.09 μm to 1.08 μm), which can be attributed to the influence caused by the AP purity.

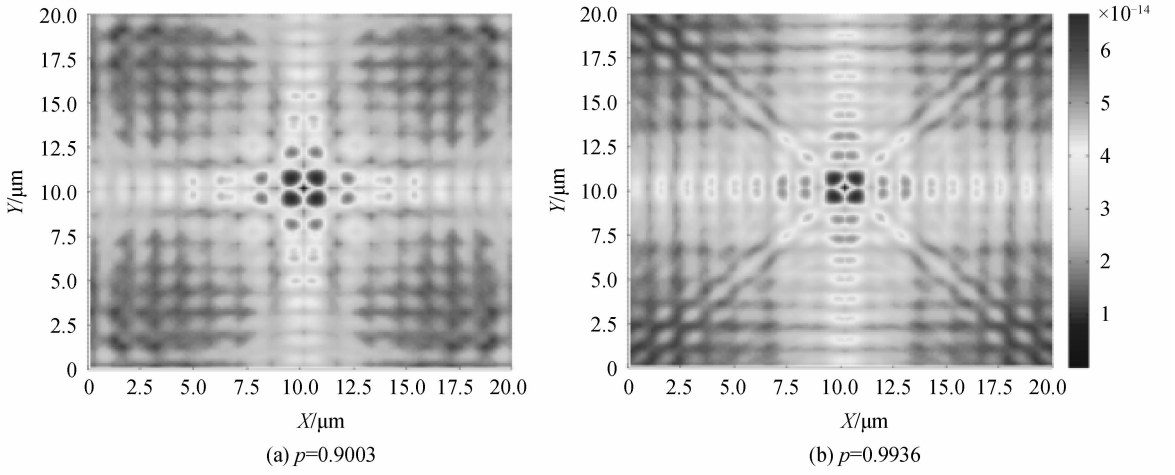

Fig. 8 Transversal component vector distributions at focal plane of different purities

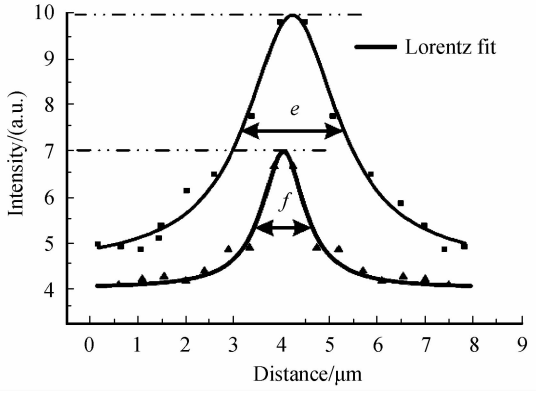

Fig. 9 Intensity distributions of the cross profile through peak of the spot in Fig. 7

Furthermore, it is expected that the femtosecond pulse be shorter, which will benefit a lot in a large sense. Take 20 fs as an example, whose RP purity is100%, oscillation frequency is 5×10^{14} Hz and Carrier Envelope Phase (CEP) is 0 respectively.

According to Fig. 10 and Fig. 11, the evolution of the electric field of the pulse can be figured out. For the longitudinal one, the intensity at the optic axis is the largest as shown in Fig. 12, and possesses a periodic change in directions, and the situation of CEP $=\pi/6$ is also shown. The distributions of the transversal one is the same. However, the intensity is zero at the pulse center.

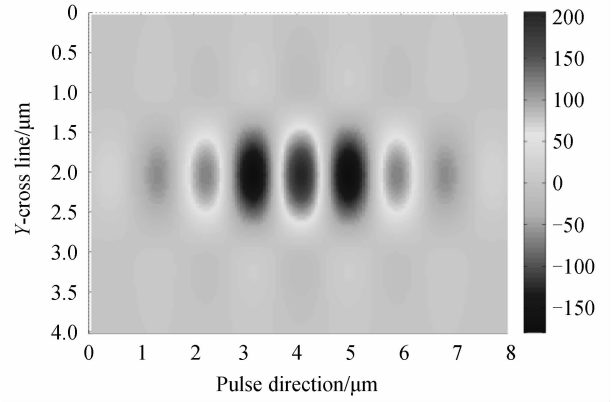

Fig. 10 Longitudinal electric field distributions of the pulse at the spot

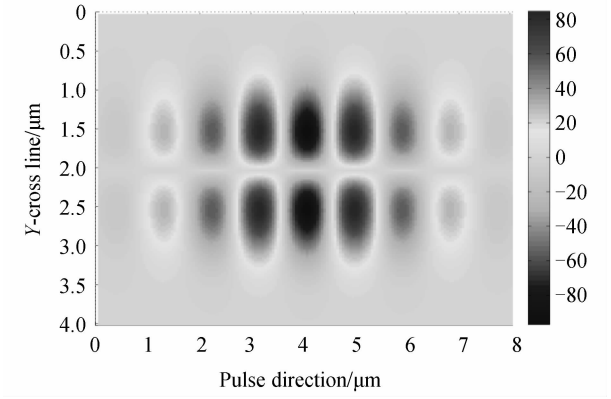

Fig. 11 Transversal electric field distributions of the pulse at the spot

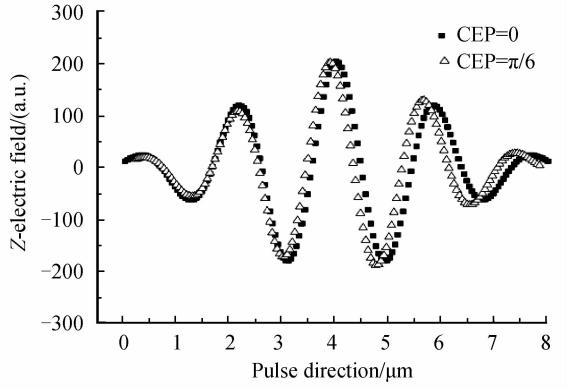

Fig. 12 Longitudinal electric field distributions along the optic axis of the pulse at the spot

Assuming that the particle concerned is electron, according to the Newton's Second Law, the velocity of the electron after interactions with the pulse at the spot can be calculated as

$$v_\tau = \int_0^\tau \frac{q_e E(t)}{m_e} \mathrm{d}t \tag{16}$$

where, τ is the pulse duration, $E(t)$ longitudinal electric fields at t moment, q_e and m_e are the charge and the mass of the electron, and Δt means subdivides of time. The expression can be further reduced as

$$v_\tau = \sum_0^n E_n \frac{q_e}{m_e} \Delta t \tag{17}$$

Thus, the results of the two CEP values can be worked out as

$$v_{\tau\,\mathrm{cep}=0} = 89.61 \frac{q_e}{m_e} \Delta t \tag{18}$$

$$v_{\tau\,\mathrm{cep}=\pi/6} = 77.61 \frac{q_e}{m_e} \Delta t \tag{19}$$

In comparison, the uniformly-polarized beams suffer from the inevitable transversal components along the optic axis when being focused, which pushes the electrons away from the areas where the longitudinal field is the largest. And the continuous one has fairly weaker peak power. Obviously, the CEP moves the position of the oscillation peak, and changes its magnitudes. As a result, the acceleration effects of the former is better, which makes controlling of the CEP be paramount for the optimum interactions.

In this process, the peak of the CW laser would firstly act on the particle on the focal spot and then the other part, while the pulse is different which meets the particle successively the heading part , the peak and last, the trailing, enjoying a Gaussian shape like the incident one. But this whole interaction would be more efficient.

This result can be illustrated by the focusing features of the pulse.

3 Conclusion

In this paper, the method to generate high peak power femtosecond few-cycle quasi-RPBs is

illustrated, and by modeling and simulations on the focal plane range, the temporal and spatial distributions of the electric field are discussed, how the RP purity affects the focusing vector features is demonstrated and the wave shape of the longitudinal components, the peak power and the vector distributions after being focused are also calculated.

Obviously, the RP sub-beams fully determine the longitudinal electrical field distributions in vector and intensity, while the transversal electrical field distributions are affected by both the AP sub-beams and the transversal components of the RP sub-beams.

Furthermore, the electric fields of different parts of the pulse after being focused are also calculated, which draft a result of the interactions between the femtosecond pulse and the electron along the axis. This work is valuable for further laser-particle interactions analysis, focusing experiments and polarization convertor design.

Reference

[1] PAYEUR S, FOURMAUX S, SCHMIDT B E, *et al*. Generation of a beam of fast electrons by tightly focusing a radially polarized ultrashort laser pulse[J]. *Applied Physics Letters*, 2012, **101**(4): 041105.

[2] MARCEAU V, APRIL A, PICHE M. Electron acceleration driven by ultrashort and non-paraxial radially polarized laser pulses[J]. *Optics Letters*, 2012, **37**(13): 2442-4.

[3] CHEN Gui-yang, SONG Feng, WANG Hua-tian. Sharper focal spot generated by 4π tight focusing of higher-order Laguerre-Gaussian radially polarized beam[J]. *Optics Letters*, 2013, **38**(19): 3937-3940.

[4] HALBAA E M, BOUSTITIB M, EZ-ZARIYA L, *et al*. Focusing properties of radially polarized modified Bessel-modulated Gaussian beam by a high numerical aperture objective[J]. *Optics & Laser Technology*, 2016, **88**: 40-53.

[5] JANET C A P, RAJESH K B, UDHAYAKUMAR M, *et al*. Tight focusing properties of radially polarized gaussian beams with pair of vortices[J]. *Chinese Physics Letters*, 2016, **33**(12): 124206.

[6] LIN Jie, CHEN Ran, YU Hai-chao, *et al*. Generation of hollow beam with radially polarized vortex beam and complex amplitude filter[J]. *Journal of the Optical Society of America*, 2014, **31**(7): 1395-1400.

[7] GU Bing, PAN Yang, WU Jia-lu, *et al*. Tight focusing properties of spatial-variant linearly-polarized vector beams[J]. *Journal of Optics*, 2014, **43**(1): 18-27.

[8] KONAWA Y, SATO S. Focusing of higher-order radially polarized Laguerre-Gaussian beam[J]. *Journal of the Optical Society of America A*, 2012, **29**(11): 2439-43.

[9] YANG Liang-xin, XIE Xiang-sheng, WANG Si-cong, *et al*. Minimized spot of annular radially polarized focusing beam [J]. *Optics Letters*, 2013, **38**(8): 1331-1333.

[10] CHEN Zi-yang, ZHAO Dao-mu. 4Pi focusing of spatially modulated radially polarized vortex beams[J]. *Optics Letters*, 2012, **37**(8): 1286-8.

[11] PRABAKARAN K, RAJESH K B, PILLAI T V S, *et al*. Generation of multiple focal spot using phase modulated radially polarized TEM11 * mode beam[J]. *Journal of Optics*, 2015, **44**(4): 311-316.

[12] ZHANG Fei, YU Hong-lin, FANG Jia-wen, *et al*. Efficient generation and tight focusing of radially polarized beam from linearly polarized beam with all-dielectric metasurface[J]. *Optics Express*, 2016, **24**(4): 6656-6664.

[13] ZHU Shi-jun, WANG Jing, LIU Xian-long, *et al*. Generation of arbitrary radially polarized array beams by manipulating correlation structure[J]. *Applied Physics Letters*, 2016, **109**(16): 161904.

[14] AGHBOLAGHI R, CHAREHJOLO H S. Radially and azimuthally polarized laser beams by thin-disk laser[J]. *Applied Optics*, 2016, **55**(13): 3510-3517.

[15] WAKAYAMA T, RODRIGUEZ-HERRERA O G, TYO J S, *et al*. Generation of achromatic, uniform-phase, radially polarized beams[J]. *Optics Express*, 2014, **22**(3): 3306-3315.

[16] MOSHE I, JACKEL S, LUMER Y, *et al*. Use of polycrystalline Nd : YAG rods to achieve pure radially or azimuthally polarized beams from high-average-power lasers[J]. *Optics Letters*, 2010, **35**(15): 2511-2513.

[17] XIE Xiang-sheng, SUN Hua-yang, YANG Liang-xin, *et al*. Effect of polarization purity of cylindrical vector beam on tightly focused spot[J]. *Journal of the Optical Society of America A*, 2013, **30**(10): 1937-40.

[18] QI Jun-li. External cavity generation and analysis of radially polarized femtosecond laser pulses[D]. Hefei: National University of Defense Technology, 2012:39-42.

[19] KHONINA S N, DEGTYAREV S A. A longitudinally polarized beam generated by a binary axicon[J]. *Journal of Russian Laser Research*, 2015, **36**(2): 151-161.

[20] HU Wen-hua. Study of key issues in super-resolution near-field structure optical storage[D]. Hefei: National University of Defense Technology, 2011: 25-27.